

Tissue Mild Extraction Enriches Membrane, Cytoplasmic, and Secreted Proteomes for Biomarker Discovery

Liangjia Du, Qianqian Hu, Jiaojiao Sha, Zijin Geng, Shanyu Qi, Ting Liu, Huimin Zhu, Dezhu Chen, Minqi Cai, Yiqiang Chen, Siyuan Liu, Hongyan Song, and Bing Bai*



Cite This: <https://doi.org/10.1021/acs.jproteome.5c00494>



Read Online

ACCESS |



Metrics & More



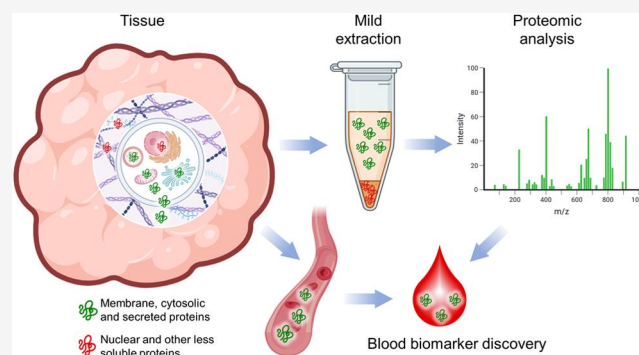
Article Recommendations



Supporting Information

ABSTRACT: Clinical blood biomarkers provide important diagnostic information and are generally secreted, cytoplasmic, membrane, and other soluble proteins. However, in the mass spectrometry-based proteomic biomarker discovery phase, the whole tissue is often lysed directly for analysis, and this increases protein complexity in the sample, limiting the detection of soluble proteins as biomarkers. Here, we use a mild extraction method that includes a low salt buffer and 1% Triton X-100 to isolate proteins from mouse tissues followed by proteomic analyses. This mild condition extracts membrane, cytoplasmic, and secreted proteins efficiently while preserving nuclear proteins largely from the mouse brain and 16 other tissues. Further in-depth proteomic analysis of the mild extract from an Alzheimer mouse brain tissue has identified more than 12,000 proteins with enrichments of soluble proteins and potential cerebrospinal fluid markers. This mild extraction has enriched membrane, cytoplasmic, and secreted proteins from tissue samples and should be used as a general method for increased success in the mass spectrometry-based proteomic discovery of circulating biomarkers.

KEYWORDS: low salt, Triton, secreted proteins, cytoplasmic proteins, membrane proteins, proteomics



INTRODUCTION

The discovery of protein biomarkers in the circulation system is important to develop blood tests in clinical laboratories for disease diagnosis and health screening. Direct profiling of proteins in plasma or serum samples can be done by recently introduced technologies like the proximity extension assays (PEAs by Olink) and the SomaScan (by SomaLogic).^{1–4} However, these antibody- or aptamer-based approaches might have questionable accuracies as specificity is a common issue in any affinity-based methodologies,⁴ and they cannot measure target proteins not defined in the libraries of their kits. In contrast, with significant developments in experimental procedures such as extensive peptide fractionation,⁵ dimethyl sulfoxide (DMSO) in liquid chromatography,⁶ data-independent acquisition-based scanning SWATH,⁷ and sophisticated mass spectrometers,⁸ the traditional liquid chromatography-mass spectrometry (LC-MS/MS) technique is progressing rapidly and has made many impressive studies in the proteomic discovery of biomarkers.^{9–14}

Because protein biomarkers released from diseased tissue lesions are diluted in the circulation system by tens to thousands of folds and their levels in the blood are often lower than the commonly abundant proteins by down to 12 orders of magnitude. This makes them difficult to be detected by the mass spectrometer even though it can detect around 5000

proteins in the plasma or serum samples now.^{15,16} Therefore, the diseased tissues that contain the enriched aberrantly expressed or modified proteins are still preferred as the starting samples for proteomic biomarker discoveries.

However, protein biomarkers such as clinically used tumor biomarkers in the blood are usually secreted, cytoplasmic, or membrane proteins (Figure S1). Nuclear proteins can occupy up to 17% of the entire cellular proteins.¹⁷ According to the Uniprot database,¹⁸ there are 2129 secreted proteins, 5756 cytoplasmic proteins, 4059 membrane proteins, and 5700 nuclear proteins in humans. The nuclear proteins plus extracellular matrix proteins in tissue samples are certainly less likely to be present in blood, but occupy a significant portion of the entire proteome. This increases the protein complexity of the samples, limiting the detection of soluble proteins that are more likely to be potential circulating biomarkers.

We initially used RIPA (radioimmunoprecipitation assay buffer) to extract these proteins from mouse brain tissues.

Received: May 24, 2025

Revised: July 15, 2025

Accepted: July 31, 2025

Although it well separated the membrane and cytosolic proteins from the nuclear proteins (Figure S2A), there were a large number of nuclear proteins coextracted in the RIPA fraction (Figure S2B,C), probably because RIPA is too strong as it contains ionic and denaturing detergents (sodium deoxycholate and sodium dodecyl sulfate). We then sought to use the milder nondenaturing detergent Triton X-100.

Triton X-100 is composed of a head of linear poly(ethylene glycol) and a tail of *p*-(2,2,4,4-tetramethylbutyl) phenol. It is a nondenaturing detergent that solubilizes lipid membranes and is widely used in biological experiments due to its desirable chemical properties. Its average molecular weight is ~630 Da as a single molecule and can assemble into micelles about 80 kDas.¹⁹ It has a low critical micelle concentration (CMC) of 0.17–0.3 mM at 25 °C and an aggregation number of 100–150 with a cloud point in low salt buffers about 64–65 °C. It also has a low hydrophilic lipophilic balance and relatively low viscosity.²⁰ Triton X-100 is a mild nonionic detergent and commonly used in extraction of membrane lipid raft proteins and other types of soluble proteins while leaving nuclear proteins largely intact.^{19,21} It is also widely used in protein extraction for mass spectrometry-based proteomic analysis.^{22–25} We have used Triton X-100 to isolate the aggregated proteins from the soluble proteins in human brain cortical tissues,^{26,27} in which we noticed that about half amount of proteins were not dissolvable by the Triton buffer, which would complicate the brain tissues if analyzed as a whole.

Here, we use the low salt buffer and the Triton detergent as the mild condition to extract secreted, cytoplasmic, and membrane proteins from tissues in an attempt to detect these soluble proteins more easily for increased successes in proteomic discoveries of circulating biomarkers.

■ EXPERIMENTAL PROCEDURES

Mice and Tissue Protein Extraction

The mice (C56BL/6J and the 5xFAD²⁸) both at the age of about 9 months were taken for tissue protein extraction. All animal experimental procedures were approved by the Ethics Committee of Nanjing Drum Tower Hospital (2025AE01048), the Affiliated Hospital of Nanjing University Medical School, and conformed to the Guide for the Care and Use of Laboratory Animals according to Chinese National Regulations.

The mouse tissues were first dissected and frozen at –80 °C. During the extraction, the frozen tissues were homogenized thoroughly in the low salt (LS) buffer (25 mM Tris–HCl, pH 7.4) with 1× protease inhibitor cocktail (PIC, Roche) by 10 mL per 1 g of tissue (this was the whole tissue lysate, WTL) and then centrifuged at 20,000g for 5 min. The supernatant was collected (the LS fraction), and the pellet was resuspended thoroughly in 1.0% Triton X-100 in the low salt buffer with 1× PIC (protease inhibitor cocktail). After centrifugation, the supernatant was harvested (the Triton fraction) and the pellet was also kept (the Pellet fraction). The LS and Triton fractions were combined (as the extract fraction) for proteomic analyses. All procedures were performed on ice.

SDS-PAGE and Western Blot

After quantification by the bicinchoninic acid method (23225, Thermo Fisher Scientific), the proteins were mixed with the 4× lithium dodecyl sulfate (LDS) sample buffer (NP0007, Thermo Fisher Scientific) to 1× and heated at 75 °C for 10 min in the presence of 10 mM dithiothreitol before being loaded to the 4–

12% gradient Bis–Tris gel (M00654, SurePAGE, Genscript) for electrophoresis and subsequent Coomassie blue staining.

After sodium dodecyl sulfate-polyacrylamide gel electrophoresis (SDS-PAGE), proteins were transferred to the nitrocellulose membrane (0.2 μm) and blocked by 5% nonfat milk in TBST buffer (50 mM Tris–HCl, pH 7.4, 100 mM NaCl, 0.05% Tween-20) for about 15 min and then incubated with primary antibodies in 3% bovine serum albumin in 1× TBST for 1 h, followed by incubation with the horseradish peroxidase-conjugated secondary antibodies in 2.5% milk. After the sample was rinsed and washed with TSBT, the chemical substrate (SuperSignal West Pico, 34087, Thermo Scientific) was used to develop signals for imaging. The primary antibodies included anti-sodium/potassium-transporting (ab300507, Abcam), anti-amyloid precursor protein (APP) (ab32136, Abcam), anti-glyceraldehyde-3-phosphate dehydrogenase (GAPDH) (60004–1, Proteintech), anti-α-tubulin (no. 2144, Cell Signaling Technology), anti-lamin B1 (ab133741, Abcam), and anti-histone H4 (ab177840, Abcam).

Protein Tryptic Digestion and Analysis by LC-MS/MS

These fraction samples were first precipitated by 80% acetonitrile and then dissolved in 8 M urea (in 25 mM TEAB, pH 8.5) with LysC at the 1/100 enzyme/protein substrate ratio for 4 h or longer at room temperature until the solution became clear. After that, 3 volumes of 25 mM TEAB (pH 8.5) were added to dilute urea to 2 M and trypsin (1/100 enzyme/substrate ratio) was added to continue the in-solution digestion. After 4–8 h at room temperature, DTT was added for reduction, followed by IAA alkylation and DTT quenching. The sample was then acidified by 1% formic acid for peptide desalting by the C18 column and dried for LC-MS/MS analysis.

In the in-depth proteomic analysis, 4 mg of digested, desalted, and dried peptides from mild extraction of the 5xFAD mouse brain tissue were resuspended in solvent A (10 mM ammonium formate, pH 8.0) and loaded onto the column (XBridge, C18, Waters, 3.5 μm resin, 4.6 × 250 mm², ~8 mg estimated loading capacity) for reverse-phase liquid chromatography (RPLC) in which were then mainly separated by 15–45% gradient of solvent B (90% AcN in solvent A, pH 8.0). About 100 fractions were collected and dried for LC-MS/MS analysis later individually without concatenation. About 1 μg peptides were loaded into the mass spectrometer (QExactive HF-X, Thermo) for about 2 h under a linear gradient of acetonitrile in the data-dependent acquisition (DDA) mode.

The MS raw data files are processed by the Proteome Discoverer 2.4 software (Thermo Fisher) and searched by the Sequest HT engine against the mouse protein database from Uniprot (UniProtKB, *Mus musculus*, reviewed, 17,230 proteins). Specific parameters are basically as the default, including full trypsin, maximum cleavages of 2, peptide length ranging from 6 to 144, 10 ppm in precursor mass tolerance and 0.02 Da in fragment ion mass tolerance, b and y ions for spectrum matching, maximum modifications of 3 and 15.995 Da (M) with N-terminal acetylation, methionine loss, or both in the dynamic modifications, and carbamidomethyl (+57.021) in the static modifications. Peptide-spectrum matches (PSMs) were verified based on *q*-values at the false discovery rate (FDR) of 1% under the Percolator module. At protein levels, the strict and relaxed FDRs were set at 1 and 5%, respectively.

All MS raw files and the search files were stored at the public server Integrated Proteome Resources iProX (<https://www.iProX.org>).

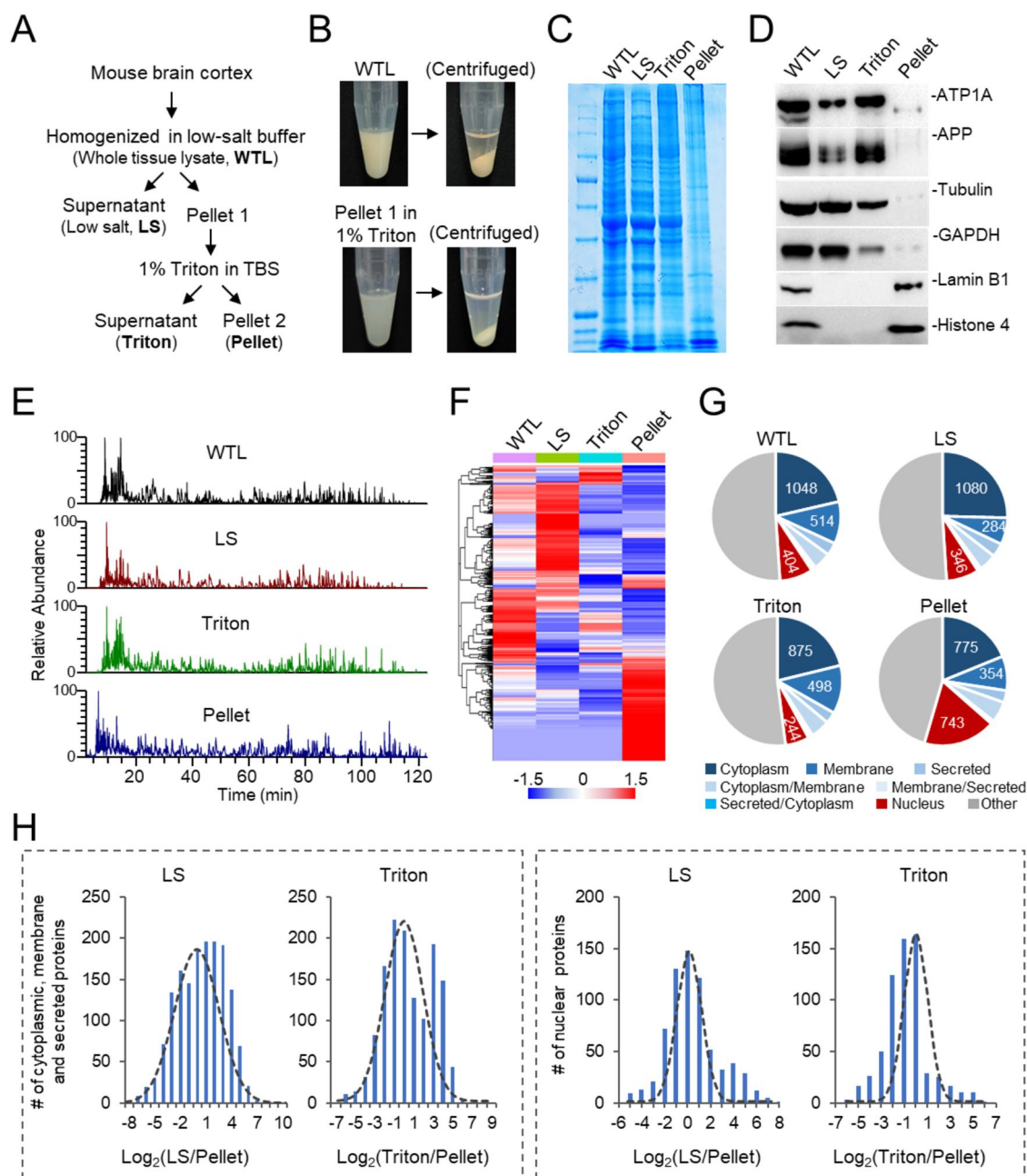


Figure 1. Mild extraction of the mouse brain tissue. (A) The workflow of the mild extraction. (B) During the extraction. (C) SDS-PAGE of the mouse brain sample and the extracts. (D) Western blots of the whole tissue lysate and extracted samples. (E) LC-MS/MS analyses of these four protein samples. (F) Heatmap analyses of the profiled proteins. (G) Distribution of protein subcellular locations in each of these four samples. (H) Enrichment analyses of the cytoplasmic and secreted proteins in the low salt and Triton extracts were performed with nuclear proteins for comparison.

iprox.cn/page/home.html),^{29,30} and the project ID is IPX0010892000 (PXD063687).

Protein Subcellular Categorization

The information on protein subcellular locations was derived from the Uniprot database (*Mus musculus*) in which there were 1509 secreted proteins, 2938 cytoplasmic proteins, 92 secreted or cytoplasmic proteins, 8848 membrane proteins, and 2545 nuclear proteins after redundant removal. Proteins identified in this study were mapped to these lists for the determination of their subcellular locations.

Protein Enrichment Analysis

The enrichment analysis was performed according to the reported.³¹ The PSM number of each protein in a sample was used for this analysis. Each PSM of a protein in a sample was first added with “1” (the minimum PSM number) to avoid zeros in the calculation of ratios between samples for \log_2 derivation. The enrichment score of each protein in two samples was calculated according to this formula: $\log_2[(\text{PSM in sample 1} + 1)/(\text{PSM in sample 2} + 1)]$. After enrichment scores of all proteins were derived, a histogram of all of these scores was made to demonstrate the distribution of frequency of proteins in different score ranges. The average of the histogram was centered at zero by subtracting the average of the entire scores

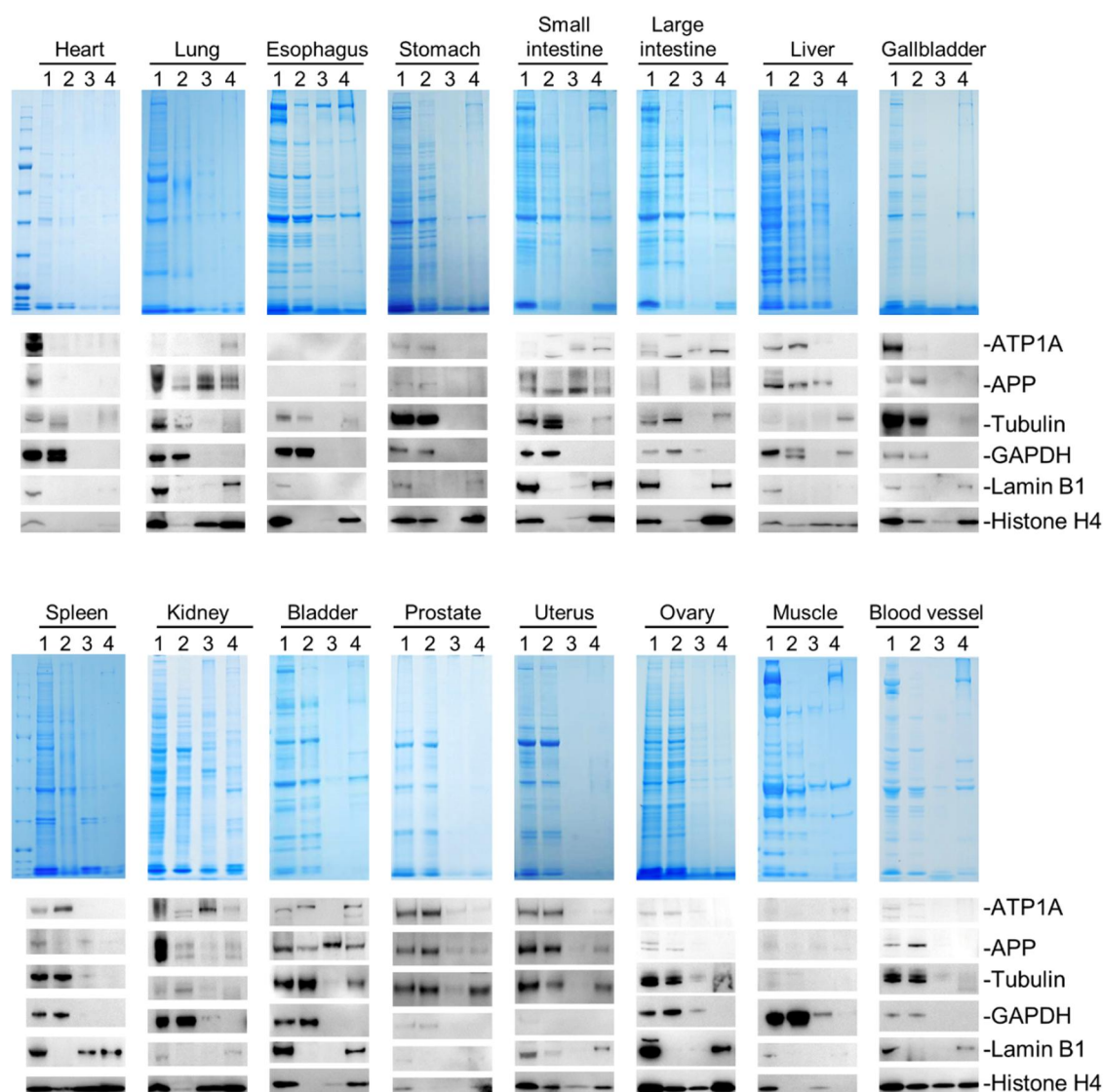


Figure 2. Mild extraction of 16 other mouse tissues demonstrated by SDS-PAGE and Western blots. ATP1A: sodium/potassium-transporting ATPase, a membrane marker. APP: amyloid- β precursor protein, a membrane protein. Tubulin and GAPDH (glyceraldehyde-3-phosphate dehydrogenase) are cytoplasmic protein markers. Lamin B1 and histone H4 are nuclear protein markers.

from the enrichment score of each protein. For example, in the first histogram of Figure 1H, the enrichment score of each protein in the LS (low salt) extract and the final undissolved pellet (Pellet) was calculated like this: $\text{Log}_2[(\text{PSM of a protein in LS} + 1)/(\text{PSM of this protein in Pellet} + 1)]$, and then all scores were taken to make the histogram with averaged centered to zero as aforementioned.

Protein Depth Analysis

For the analysis of protein depth in serum, the serum proteins were downloaded from the reported study¹⁶ and the Human Protein Atlas database⁴ and ranked according to their relative abundance (PSM numbers) or their absolute concentrations (ng/L) from high to low levels.

Protein Cellular Component, Molecular Function, and Biological Process Analyses

The cellular component enrichment analysis was performed with the The Database for Annotation, Visualization, and Integrated Discovery (DAVID) analysis tool available on the National Institutes of Health website under defaulted parameter

settings. Results with significant *P* values, Bonferroni values, Benjamini values, and false discovery rates were simultaneously selected.

RESULTS

Mild Extraction of the Mouse Brain Tissue

We first determined the optimal concentration of Triton X-100 for extraction using mouse brain tissue and found that 1.0% is able to extract proteins sufficiently (Figure S3). In the extraction, the brain tissue was first homogenized in the low salt buffer (whole tissue lysate, WTL) and then separated after centrifuge into the supernatant (the LS fraction) and the pellet. The pellet was further dissolved by 1% Triton in the low salt buffer and then centrifuged into the supernatant (the Triton fraction) and the final pellet (the pellet fraction) (Figure 1A,B). By SDS-PAGE, the proteins were largely extracted in the LS and Triton fractions, which also showed distinct patterns from the proteins in the pellet fraction (Figure 1C). The Western blots demonstrated that the membrane proteins (ATP1A and APP) and cytoplasmic proteins (tubulin and GAPDH) were enriched

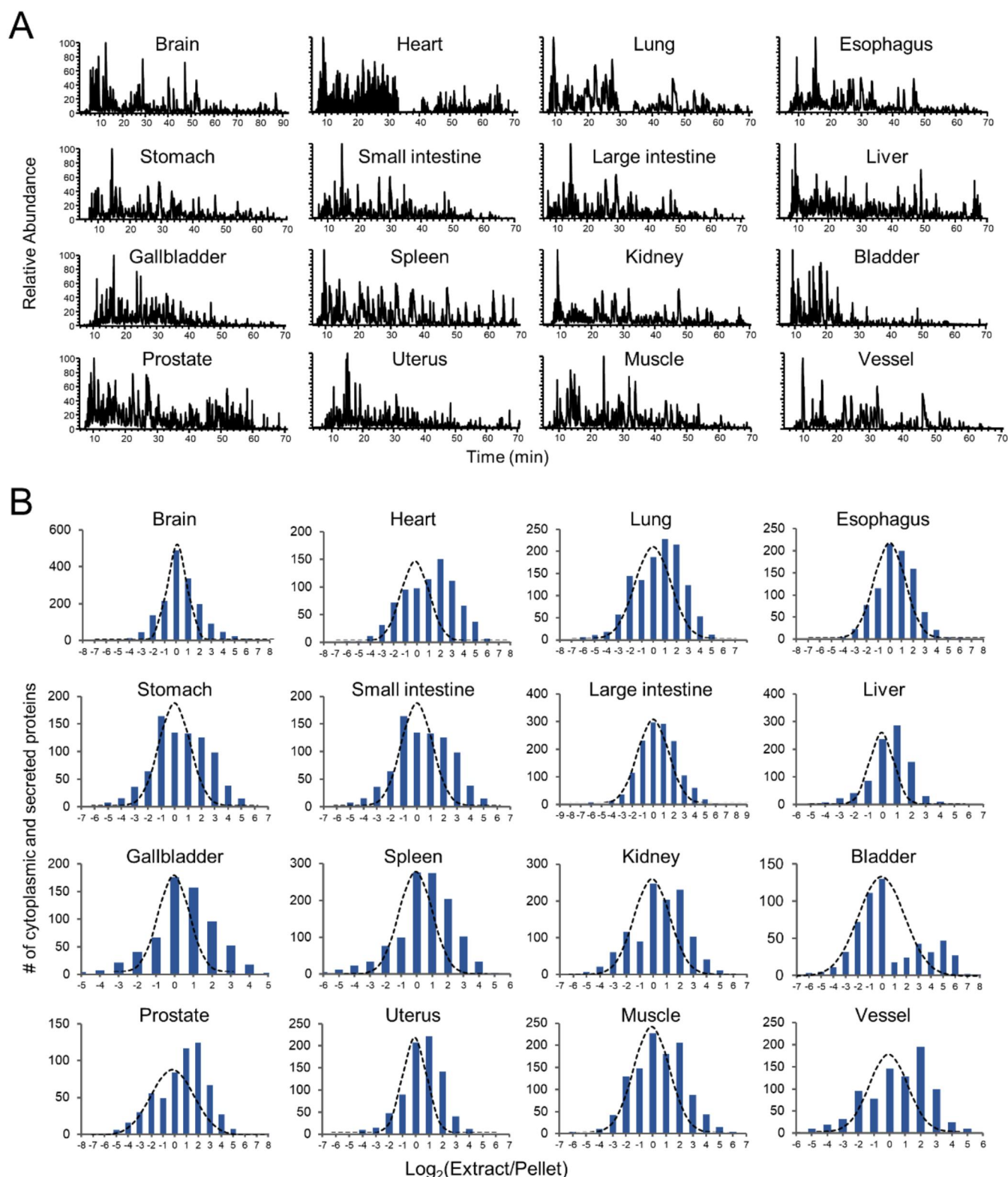


Figure 3. Mild extraction of 16 mouse tissues. (A) LC-MS/MS analyses of the mild extract samples. The low salt and Triton fractions were combined for the proteomic analyses. (B) Enrichment analyses of the cytoplasmic and secreted proteins. Extract: combined LS and Triton fractions.

in the LS and Triton fractions, while the nuclear proteins (histone H4 and lamin B1) remained mainly in the pellet fraction as expected (Figure 1D).

The four samples (WTL, LS, Triton, and pellet) were then analyzed by LC-MS/MS. The liquid chromatographs of the LS and Triton extracts were similar to that of WTL while the pellet

showed a distinct pattern (Figure 1E), consistent with the previous results (Figure 1C,D). The heatmap analysis demonstrated clearly that the LS and Triton fractions enriched different subsets of proteins from what the pellet fractions enriched (Figure 1F). There were 1080 and 875 cytoplasmic proteins, 284 and 498 membrane proteins in the LS and Triton

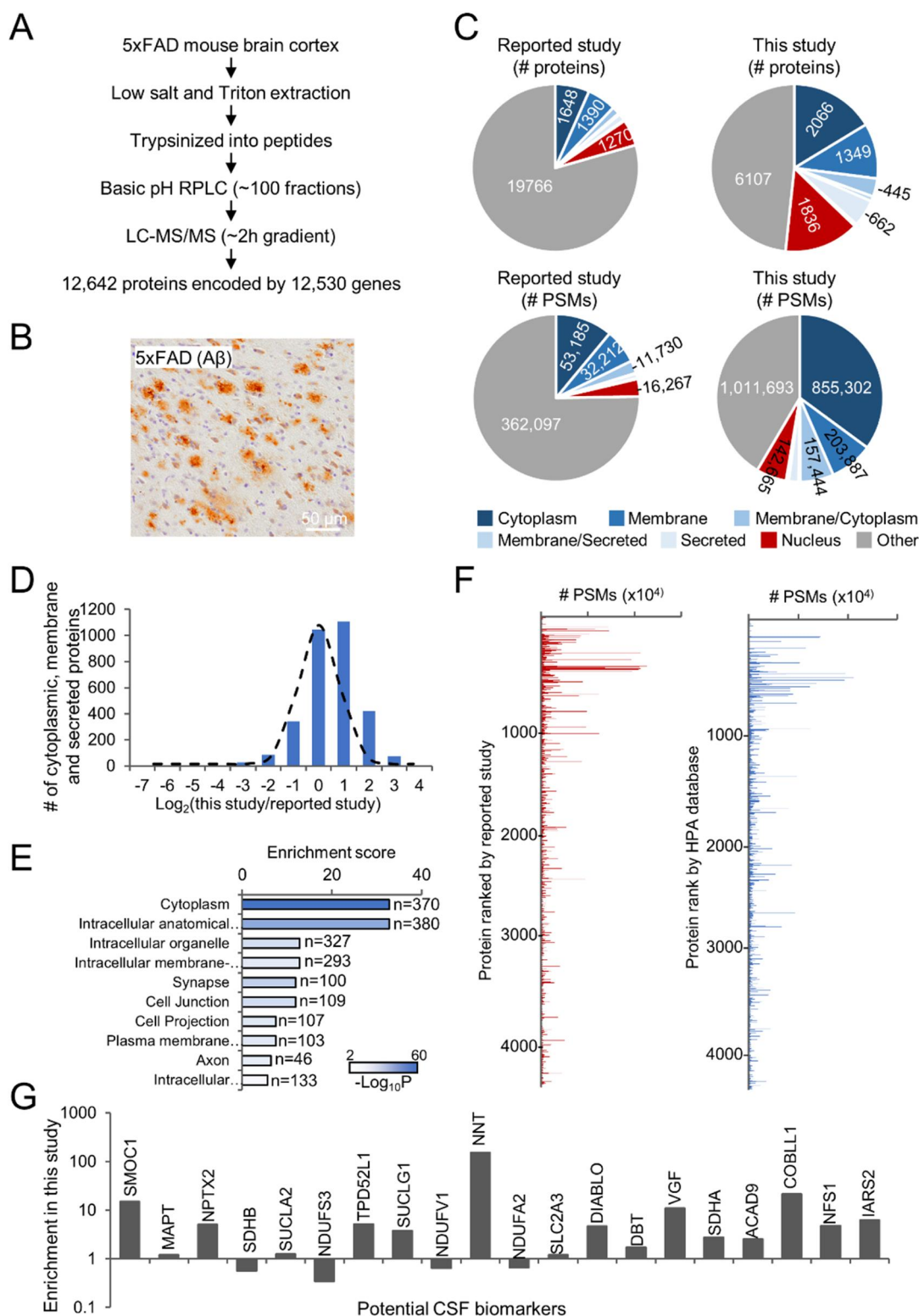


Figure 4. Mild extract and in-depth proteomic analysis of the brain cortical tissue of an Alzheimer mouse. (A) The workflow of the extraction and the deep proteomic analysis. 5xFAD: a widely used Alzheimer mouse model. (B) The immunohistochemical staining of the selected mouse brain. Antibody: anti-A β (6E10). (C) The numbers of cytoplasmic, membrane, secreted, and nuclear proteins and PSMs identified in this study and the reported study by Dr. Peng in which the whole mouse cortical tissues were homogenized in lysis buffer with 8 M urea (in 50 mM HEPES, pH 8.5, 0.5% sodium deoxycholate). (D) Enrichment analysis of the proteins identified in this study compared with the report by Dr. Peng. Log₂Ratios of protein PSMs in both studies were taken for analysis. Proteins encoded by 8335 genes were identified in both studies. (E) DAVID cellular component analysis of the top 5% increased proteins ($n = 416$) of this study compared to the reported study. (F) Identified proteins in this study are ranked by the reported study and the Human Protein Atlas (HPA) database. (G) Enrichment analysis of potential AD CSF biomarkers. The levels (MS signal intensity or PSM) of each of these proteins were divided by the level of histone H4 (as the control) in the reported study or this study, and the ratio of the relative levels of each protein in this study and the reported study was taken.

fractions, similar to the numbers in the WTL (1048 and 514), but only 775 cytoplasmic proteins and 354 membrane proteins in the pellet. In contrast, the pellet had 743 nuclear proteins, much more than in the WTL, LS, and Triton samples (Figure 1G). These suggest that the low salt and Triton solutions extract most of the soluble proteins while resisting nuclear proteins.

Indeed, compared to the pellet, both LS and Triton fractions enriched cytoplasmic and secreted proteins, as demonstrated by additional numbers of these proteins projected out on the positive side of the normal distribution of $\text{Log}_2(\text{LS}/\text{Pellet})$ or $\text{Log}_2(\text{Triton}/\text{Pellet})$ values; in contrast, for the nuclear proteins, the distribution of the Log_2 -ratios between the LS or Triton and the pellet biased to the left side, suggesting a resistance of this type of proteins in the LS and Triton fractions (Figure 1H).

Mild Extraction of 16 Other Mouse Tissues and Proteomic Analyses

We further examined whether this mild extraction method could be expanded to other types of tissues, including heart, lung, esophagus, stomach, small and large intestines, liver, gallbladder, spleen, kidney, bladder, prostate, uterus, ovary, muscle, and blood vessels. Similar to the brain extraction, the LS and Triton had largely extracted the proteins from the whole tissue lysate and proteins left in the pellet showed generally distinct patterns on SDS-PAGEs (Figure 2). Consistently, the membrane and cytoplasmic protein markers were enriched in the LS and Triton fractions, while the two nuclear protein markers, lamin B1 and histone H4, remained in the pellet fractions of most tissue samples (Figures 2 and S4). These data suggested that the mild extraction strategy was also able to enrich soluble proteins efficiently in these tissues.

Because both LS and Triton fractions had extracted soluble proteins, we therefore combined them as the extract fraction and performed proteomic analysis together with WTL and pellet fractions. For all 16 tissue samples, the liquid chromatographs of the extract were generally similar to those of their WTL samples but distinct from those of the pellet samples (Figures 3A and S5). Proteins were well isolated in the extract and the pellet fractions (Figure S6 and Table S1). The enrichment analyses showed enrichments of cytoplasmic and secreted proteins in the extract fraction for almost all 16 tissue samples (Figure 3B). About 80% of the proteins with defined subcellular locations were membrane, cytoplasmic, or secreted proteins, and around 20% were nuclear proteins (Figure S7).

To further look into the solubility of proteins among different tissues, we took the top 5% most enriched proteins compared to the whole tissue lysate from each tissue and performed the gene ontology analyses. The results showed that the enriched cellular components, molecular functions, and biological processes were largely different from one another among these 16 tissues (Figure S8A–C). This is probably because of the differences in the protein expression and modifications, association with other proteins or molecules, and molecular complexity of the tissues.

We also noticed that nuclear proteins could be found in the soluble extract. In the top 2.5% most enriched proteins in the extract fraction of each tissue, nuclear proteins ranged from 22.8% (28 out of a total of 123 proteins identified) in the brain to none in the heart tissue (Figure S9A). Among all nuclear proteins enriched in the soluble extract of the 16 tissues, some were histones, and others were involved in DNA or RNA binding, transporting, processing, regulation, or other processes (Figure S9B). Gene ontology analyses showed enrichments in particular cellular components, molecular functions, and

biological processes, but the number of proteins in each enrichment was small (Figure S9C). The observation of enrichment of nuclear proteins in the soluble extract is probably because they are under protein synthesis in the cytosol. It is also because some proteins (such as Nup210) are nuclear pore membrane proteins that are released in the presence of Triton. Secretion of nuclear proteins is another important possible reason for this observation.³²

In-Depth Proteomic Analysis of an Alzheimer Mouse Brain Tissue

To further examine the mild extraction efficiency, we took the brain cortical tissue from an Alzheimer mouse named 5xFAD²⁸ and performed a deep proteomic analysis on the mild extract (Figure 4A). This transgenic mouse bears five mutations on two familial Alzheimer genes APP and PSEN1 and demonstrates the hallmark of A β amyloid plaques (Figure 4B) in human patients with Alzheimer's disease (AD).²⁸ We chose this mouse model because we already performed ultradeep proteome analyses of both AD and 5xFAD brain cortices³³ and also of the AD serum samples, which could be used for comparison in this study.¹⁶

The deep proteomic analysis identified 2066 cytoplasmic proteins and 1349 membrane proteins, more than the reported 1648 cytoplasmic proteins and 1390 membrane proteins in the study,³³ which used the whole mouse cortical tissue (Figure 4C and Table S2), and also more than the profiled mouse brain proteins in a recent report³⁴ (Figure S10). To be more precise, we looked into the mass-spectrometric (MS) scans of the analyses and found that a much higher proportion of the scans were matched to the peptides of cytoplasmic, membrane, and secreted proteins in our study (Figure 4C). The enrichment analysis also showed prominently extra MS scans mapped to peptides from cytoplasmic, membrane, and secreted proteins (Figure 4D).

We compared the levels of all proteins identified in our study and the reported study and took the top 5% of the increased proteins for cellular component analysis. The results showed that these proteins were enriched in cytoplasm, membrane, or membranous organelles (Figure 4E), suggesting again the enrichment of soluble proteins in our mild extraction.

We next mapped all proteins identified in this deep proteomic analysis to the serum proteins from the report and the Human Protein Atlas database and found that proteins at the lowest levels (~ 1.0 pg/mL) could be detected by this in-depth proteomic analysis (Figure 4F).

We also looked at particular proteins that were reported to be potential AD CSF markers^{33,35} and found that most of these proteins were enriched in our study (Figure 4G), suggesting an increased chance of being detected by mild extraction.

DISCUSSION

In this study, we used low salt buffer and Triton to extract mouse brain and 16 other tissues, which have enriched membrane, cytoplasmic, and secreted proteins that can be released into the peripheral blood system as clinical biomarkers, increasing the chances of success in the mass spectrometry-based proteomic discoveries of plasma or serum biomarkers.

The nuclear proteins are largely resistant to Triton X-100, probably because Triton can only strip the outer membrane of the nuclear envelope,³⁶ leaving nuclear proteins in a large amount inside the inner membrane. In fact, Triton X-100 was used to extract nuclear proteins as they were enriched in the

pellet resistant to it,^{37–39} confirming the effect of Triton to spare nuclear proteins.

Using this mild extraction method, we found that many brain disease biomarkers were actually enriched remarkably. When normalized by histone H4 in the sample, the relative levels of potential brain disease biomarkers in blood,^{40–43} such as APP and MAPT (hallmark proteins of Alzheimer's disease), NEFL (brain injury), GFAP (glial damage), UCH-L1/NSE/Copeptin (neuronal damage), S100 β (astroglia), and SNTF (axonal injury) could increase by several or more folds in the LS fraction and by up to 25-folds in the Triton fraction as compared to the whole tissue lysate analyzed as a whole without extraction (Figure S11), strongly suggesting the high efficiency of the mild extraction for circulating biomarker discoveries.

In addition, under proteomic analyses of all of these mouse tissues, some tissue-specific proteins could be found. For example, in addition to Nefm, Nefl, and Map2, other proteins like Slc1a2, protein bassoon, synaptotagmin-1, and synapsin-1 were also specifically and highly present in the brain (Figure S12 and Table S1). Moreover, in the heart tissue, besides troponin I, T, and C that are now widely used, clinical myocardial infarction markers Myl2 and Mybpc3 are also abundant and enriched in the heart tissue. All tissue-specific and plentiful proteins such as these identified in this study could be considered potential blood markers when these tissues are damaged.

It is necessary to mention that Triton X-100 is a mild nonionic detergent, which is not able to solubilize proteins integrated in the cell membrane lipid rafts and is hard to dissociate proteins tightly attached to other less soluble matrices or molecular complexes through ionic interactions. These proteins might be spun down to the pellet during centrifugation, causing incomplete extraction of these proteins in the soluble fraction. This is probably one of the reasons that the membrane, cytosolic proteins, and other soluble proteins can also be seen in a certain amount in the pellet fraction in this study (Figures 2, S4, and S7 and Table S1). Nevertheless, proteins are usually not always 100% integrated or attached. Even a small fraction of these proteins in more free forms can be detected, especially when in-depth mass spectrometry-based proteomic analyses are performed.

Overall, the mild extraction of tissue protein samples by low salt buffer and Triton might be an efficient approach for the mass spectrometry-based proteomic discoveries of peripheral circulating biomarkers.

■ ASSOCIATED CONTENT

Data Availability Statement

All MS raw files and the search files were stored at the public server Integrated Proteome Resources iProX (<https://www.iprox.cn/page/home.html>)^{29,30}, and the project ID is IPX0010892000 (PXD063687).

SI Supporting Information

The Supporting Information is available free of charge at <https://pubs.acs.org/doi/10.1021/acs.jproteome.5c00494>.

Common tumor biomarkers and their subcellular locations (Figure S1); extraction of mouse brain tissue by RIPA buffer (Figure S2); determination of optimal concentrations and repeated extraction times (Figure S3); original Western blots for Figures 1 D and 2 B (Figure S4); the liquid chromatographs of LC-MS/MS analyses of 16 mouse tissues (Figure S5); heatmap analyses of the

levels of the identified proteins in the whole tissue lysate and the extracts of each mouse tissue (Figure S6); the distribution of membrane, cytoplasmic, secreted, and nuclear proteins identified in the extract fraction sample (Figure S7); the gene ontology analyses of the enriched proteins in the extract fraction of each tissue (Figure S8); different subcellular categories of the top 2.5% enriched proteins in the Triton fraction (Figure S9); composition of proteins in different subcellular locations in a recent report (Figure S10); enrichment of potential brain disease protein markers in the LS and Triton fractions of the mouse brain tissue lysate (Figure S11); and the relative levels of each protein identified in the 16 mouse tissues (Figure S12) (PDF)

Proteomic analyses of 16 mouse tissue mild extracts (Table S1) (XLSX)

In-depth proteomic analysis of 5xFAD mouse brain tissue mild extract (Table S2) (XLSX)

■ AUTHOR INFORMATION

Corresponding Author

Bing Bai – Department of Laboratory Medicine, Nanjing Drum Tower Hospital Clinical College of Nanjing Normal University, Nanjing, Jiangsu 210008, China; Department of Laboratory Medicine, Nanjing Drum Tower Hospital Clinical College of Nanjing University of Chinese Medicine, Nanjing, Jiangsu 210008, China; Department of Laboratory Medicine, Nanjing Drum Tower Hospital, Affiliated Hospital of Medical School, Nanjing University, Nanjing, Jiangsu 210008, China; orcid.org/0009-0002-1505-2965; Email: bing.bai@nju.edu.cn

Authors

Liangjia Du – Department of Laboratory Medicine, Nanjing Drum Tower Hospital Clinical College of Nanjing Normal University, Nanjing, Jiangsu 210008, China
Qianqian Hu – Department of Laboratory Medicine, Nanjing Drum Tower Hospital Clinical College of Nanjing Normal University, Nanjing, Jiangsu 210008, China
Jiaojiao Sha – Department of Laboratory Medicine, Nanjing Drum Tower Hospital Clinical College of Nanjing University of Chinese Medicine, Nanjing, Jiangsu 210008, China
Zijin Geng – Department of Laboratory Medicine, Nanjing Drum Tower Hospital Clinical College of Nanjing University of Chinese Medicine, Nanjing, Jiangsu 210008, China
Shanyu Qi – Department of Laboratory Medicine, Nanjing Drum Tower Hospital Clinical College of Nanjing Medical University, Nanjing 210008, China
Ting Liu – Department of Laboratory Medicine, Nanjing Drum Tower Hospital Clinical College of Nanjing Medical University, Nanjing 210008, China
Huimin Zhu – Chemistry and Biomedicine Innovation Center, Medical School of Nanjing University, Nanjing, Jiangsu 210008, China
Dezhu Chen – Department of Nuclear Medicine, Nanjing Drum Tower Hospital, Affiliated Hospital of Medical School, Nanjing University, Nanjing, Jiangsu 210008, China
Minqi Cai – Department of Nuclear Medicine, Nanjing Drum Tower Hospital, Affiliated Hospital of Medical School, Nanjing University, Nanjing, Jiangsu 210008, China

Yiqiang Chen — Center for Precision Medicine, Nanjing Drum Tower Hospital, Affiliated Hospital of Medical School, Nanjing University, Nanjing, Jiangsu 210008, China

Siyuan Liu — Center for Precision Medicine, Nanjing Drum Tower Hospital, Affiliated Hospital of Medical School, Nanjing University, Nanjing, Jiangsu 210008, China

Hongyan Song — Department of Laboratory Medicine, Nanjing Drum Tower Hospital, Affiliated Hospital of Medical School, Nanjing University, Nanjing, Jiangsu 210008, China

Complete contact information is available at:

<https://pubs.acs.org/10.1021/acs.jproteome.5c00494>

Author Contributions

Conceptualization: B.B.; methodology: L.D., Q.H., J.S., Z.G., S.Q., T.L., and H.Z.; validation: L.D., Q.H., D.C., M.C., Y.C., S.L., and H.S.; formal analysis: L.D., Q.H., and B.B.; investigation: L.D. and B.B.; data curation: L.D., Q.H., and B.B.; writing and editing: all authors; project administration: B.B.; and funding acquisition: B.B.

Notes

The authors declare no competing financial interest.

ACKNOWLEDGMENTS

This work was supported by the National Natural Science Foundation of China (82172354, 82472333 to B.B.), the Research Foundation of Jiangsu Provincial Commission of Health and Family Planning (M2021012 to B.B.), the Nanjing Medical Science and Technology Development Foundation (ZKX22013 to B.B.), the fundings for Novel Technology and Clinical Trials from the Affiliated Drum Tower Hospital, Medical School of Nanjing University (XJSFZLX202331 and 2022-LCYJ-MS-02 to B.B.).

REFERENCES

- (1) Eldjarn, G. H.; Ferkingstad, E.; Lund, S. H.; Helgason, H.; Magnusson, O. T.; Gunnarsdottir, K.; Olafsdottir, T. A.; Halldorsson, B. V.; Olason, P. I.; Zink, F.; et al. Large-scale plasma proteomics comparisons through genetics and disease associations. *Nature* **2023**, 622 (7982), 348–358.
- (2) Ferkingstad, E.; Sulem, P.; Atlason, B. A.; Sveinbjornsson, G.; Magnusson, M. I.; Styrudsdottir, E. L.; Gunnarsdottir, K.; Helgason, A.; Oddsson, A.; Halldorsson, B. V.; et al. Large-scale integration of the plasma proteome with genetics and disease. *Nat. Genet.* **2021**, 53 (12), 1712–1721.
- (3) Oh, H.-H.; Rutledge, J.; Nachun, D.; Palovics, R.; Abiose, O.; Moran-Losada, P.; Channappa, D.; Urey, D. Y.; Kim, K.; Sung, Y. J.; et al. Organ aging signatures in the plasma proteome track health and disease. *Nature* **2023**, 624 (7990), 164–172.
- (4) Deutsch, E. W.; Omenn, G. S.; Sun, Z.; Maes, M.; Pernemalm, M.; Palaniappan, K. K.; Letunica, N.; Vandenbrouck, Y.; Brun, V.; Tao, S. C.; et al. Advances and Utility of the Human Plasma Proteome. *J. Proteome Res.* **2021**, 20 (12), 5241–5263.
- (5) Zhang, X.; Sun, H.; Wang, Z.; Zhou, S.; Fu, Y.; Anthony, H. A.; Peng, J. In-Depth Blood Proteome Profiling by Extensive Fractionation and Multiplexed Quantitative Mass Spectrometry. *Methods Mol. Biol.* **2023**, 2628, 109–125.
- (6) Hahne, H.; Pachi, F.; Ruprecht, B.; Maier, S. K.; Klaeger, S.; Helm, D.; Medard, G.; Wilm, M.; Lemeer, S.; Kuster, B. DMSO enhances electrospray response, boosting sensitivity of proteomic experiments. *Nat. Methods* **2013**, 10 (10), 989–991.
- (7) Messner, C. B.; Demichev, V.; Bloomfield, N.; Yu, J. S. L.; White, M.; Kreidl, M.; Egger, A. S.; Freiwald, A.; Ivoisev, G.; Wasim, F.; et al. Ultra-fast proteomics with Scanning SWATH. *Nat. Biotechnol.* **2021**, 39 (7), 846–854.
- (8) Heil, L. R.; Damoc, E.; Arrey, T. N.; Pashkova, A.; Denisov, E.; Petzoldt, J.; Peterson, A. C.; Hsu, C.; Searle, B. C.; Shulman, N.; et al. Evaluating the Performance of the Astral Mass Analyzer for Quantitative Proteomics Using Data-Independent Acquisition. *J. Proteome Res.* **2023**, 22 (10), 3290–3300.
- (9) Malmström, E.; Malmstrom, L.; Hauri, S.; Mohanty, T.; Scott, A.; Karlsson, C.; Gueto-Tettay, C.; Ahlman, E.; Nozohoor, S.; Tingstedt, B.; et al. Human proteome distribution atlas for tissue-specific plasma proteome dynamics. *Cell* **2025**, 188, 2810–2822.e16.
- (10) Guo, T.; Steen, J. A.; Mann, M. Mass-spectrometry-based proteomics: from single cells to clinical applications. *Nature* **2025**, 638 (8052), 901–911.
- (11) Nakayasu, E. S.; Gritsenko, M.; Piehowski, P. D.; Gao, Y.; Orton, D. J.; Schepmoes, A. A.; Fillmore, T. L.; Frohnert, B. I.; Rewers, M.; Krischer, J. P.; et al. Tutorial: best practices and considerations for mass-spectrometry-based protein biomarker discovery and validation. *Nat. Protoc.* **2021**, 16 (8), 3737–3760.
- (12) Niu, L.; Thiele, M.; Geyer, P. E.; Rasmussen, D. N.; Webel, H. E.; Santos, A.; Gupta, R.; Meier, F.; Strauss, M.; Kjaergaard, M.; et al. Noninvasive proteomic biomarkers for alcohol-related liver disease. *Nat. Med.* **2022**, 28 (6), 1277–1287.
- (13) Khoo, A.; Liu, L. Y.; Nyalwidhe, J. O.; Semmes, O. J.; Vesprini, D.; Downes, M. R.; Boutros, P. C.; Liu, S. K.; Kislinger, T. Proteomic discovery of non-invasive biomarkers of localized prostate cancer using mass spectrometry. *Nat. Rev. Urol.* **2021**, 18 (12), 707–724.
- (14) Åkesson, J.; Hojjati, S.; Hellberg, S.; Raffetseder, J.; Khademi, M.; Rynkowski, R.; Kockum, I.; Altafini, C.; Lubovac-Pilav, Z.; Møllergaard, J.; et al. Proteomics reveal biomarkers for diagnosis, disease activity and long-term disability outcomes in multiple sclerosis. *Nat. Commun.* **2023**, 14 (1), No. 6903.
- (15) Keshishian, H.; Burgess, M. W.; Specht, H.; Wallace, L.; Clauser, K. R.; Gillette, M. A.; Carr, S. A. Quantitative, multiplexed workflow for deep analysis of human blood plasma and biomarker discovery by mass spectrometry. *Nat. Protoc.* **2017**, 12 (8), 1683–1701.
- (16) Dey, K. K.; Wang, H.; Niu, M.; Bai, B.; Wang, X.; Li, Y.; Cho, J. H.; Tan, H.; Mishra, A.; High, A. A.; et al. Deep undepleted human serum proteome profiling toward biomarker discovery for Alzheimer's disease. *Clin. Proteomics* **2019**, 16, No. 16.
- (17) Fink, J. L.; Karunaratne, S.; Mittal, A.; Gardiner, D. M.; Hamilton, N.; Mahony, D.; Kai, C.; Suzuki, H.; Hayashizaki, Y.; Teasdale, R. D. Towards defining the nuclear proteome. *Genome Biol.* **2008**, 9 (1), No. R15.
- (18) Bateman, A.; Martin, M. J.; Orchard, S.; et al. UniProt: the Universal Protein Knowledgebase in 2023. *Nucleic Acids Res.* **2023**, 51 (D1), D523–D531.
- (19) Linke, D. Detergents. In *Methods in Enzymology*; Elsevier, 2009; Chapter 34, Vol. 463, pp 603–617.
- (20) Yadav, V.; Lunson, M.; Shore, H.; Aucamp, J. Systematic Development of a Detergent Toolbox as an Alternative to Triton X-100. *Biotechnol. Bioeng.* **2025**, 122 (5), 1096–1104.
- (21) Das, A.; Bysack, A.; Raghuraman, H. Effectiveness of dual-detergent strategy using Triton X-100 in membrane protein purification. *Biochem. Biophys. Res. Commun.* **2021**, 578, 122–128.
- (22) Cox, B.; Emili, A. Tissue subcellular fractionation and protein extraction for use in mass-spectrometry-based proteomics. *Nat. Protoc.* **2006**, 1 (4), 1872–1878.
- (23) Christopher, J. A.; Stadler, C.; Martin, C. E.; Morgenstern, M.; Pan, Y.; Betsinger, C. N.; Ratray, D. G.; Mahdessian, D.; Gingras, A. C.; Warscheid, B.; et al. Subcellular proteomics. *Nat. Rev. Methods Primers* **2021**, 1, No. 32, DOI: 10.1038/s43586-021-00029-y.
- (24) Hughes, C. S.; Moggridge, S.; Muller, T.; Sorensen, P. H.; Morin, G. B.; Krijgsvelde, J. Single-pot, solid-phase-enhanced sample preparation for proteomics experiments. *Nat. Protoc.* **2019**, 14 (1), 68–85.
- (25) Isaacson, T.; Damasceno, C. M.; Saravanan, R. S.; He, Y.; Catala, C.; Saladie, M.; Rose, J. K. Sample extraction techniques for enhanced proteomic analysis of plant tissues. *Nat. Protoc.* **2006**, 1 (2), 769–774.
- (26) Bai, B.; Hales, C. M.; Chen, P. C.; Gozal, Y.; Dammer, E. B.; Fritz, J. J.; Wang, X.; Xia, Q.; Duong, D. M.; Street, C.; et al. U1 small nuclear

ribonucleoprotein complex and RNA splicing alterations in Alzheimer's disease. *Proc. Natl. Acad. Sci. U.S.A.* **2013**, *110* (41), 16562–16567.

(27) Chen, P. C.; Han, X.; Shaw, T. I.; Fu, Y.; Sun, H.; Niu, M.; Wang, Z.; Jiao, Y.; Teubner, B. J. W.; Eddins, D.; et al. Alzheimer's disease-associated U1 snRNP splicing dysfunction causes neuronal hyperexcitability and cognitive impairment. *Nat. Aging* **2022**, *2* (10), 923–940.

(28) Oakley, H.; Cole, S. L.; Logan, S.; Maus, E.; Shao, P.; Craft, J.; Guillozet-Bongaarts, A.; Ohno, M.; Disterhoft, J.; Van Eldik, L.; et al. Intraneuronal beta-amyloid aggregates, neurodegeneration, and neuron loss in transgenic mice with five familial Alzheimer's disease mutations: potential factors in amyloid plaque formation. *J. Neurosci.* **2006**, *26* (40), 10129–10140.

(29) Ma, J.; Chen, T.; Wu, S.; Yang, C.; Bai, M.; Shu, K.; Li, K.; Zhang, G.; Jin, Z.; He, F.; et al. iProX: an integrated proteome resource. *Nucleic Acids Res.* **2019**, *47* (D1), D1211–D1217.

(30) Chen, T.; Ma, J.; Liu, Y.; Chen, Z.; Xiao, N.; Lu, Y.; Fu, Y.; Yang, C.; Li, M.; Wu, S.; et al. iProX in 2021: connecting proteomics data sharing with big data. *Nucleic Acids Res.* **2022**, *50* (D1), D1522–D1527.

(31) Zaman, M.; Fu, Y.; Chen, P. C.; Sun, H.; Yang, S.; Wu, Z.; Wang, Z.; Poudel, S.; Serrano, G. E.; Beach, T. G.; et al. Dissecting Detergent-Insoluble Proteome in Alzheimer's Disease by TMTc-Corrected Quantitative Mass Spectrometry. *Mol. Cell. Proteomics* **2023**, *22* (8), No. 100608.

(32) Nickel, W.; Rabouille, C. Mechanisms of regulated unconventional protein secretion. *Nat. Rev. Mol. Cell Biol.* **2009**, *10* (2), 148–155.

(33) Bai, B.; Wang, X.; Li, Y.; Chen, P. C.; Yu, K.; Dey, K. K.; Yarbrow, J. M.; Han, X.; Lutz, B. M.; Rao, S.; et al. Deep Multilayer Brain Proteomics Identifies Molecular Networks in Alzheimer's Disease Progression. *Neuron* **2020**, *105* (6), 975–991 e7.

(34) Li, W.; Dasgupta, A.; Yang, K.; Wang, S.; Hemandhar-Kumar, N.; Chepyala, S. R.; Yarbrow, J. M.; Hu, Z.; Salovska, B.; Fornasiero, E. F.; et al. Turnover atlas of proteome and phosphoproteome across mouse tissues and brain regions. *Cell* **2025**, *188* (8), 2267–2287 .e21.

(35) Bai, B.; Vanderwall, D.; Li, Y.; Wang, X.; Poudel, S.; Wang, H.; Dey, K. K.; Chen, P. C.; Yang, K.; Peng, J. Proteomic landscape of Alzheimer's Disease: novel insights into pathogenesis and biomarker discovery. *Mol. Neurodegener.* **2021**, *16* (1), No. 55.

(36) Schirmer, E. C.; Gerace, L. The nuclear membrane proteome: extending the envelope. *Trends Biochem. Sci.* **2005**, *30* (10), 551–558.

(37) Dreger, M.; Bengtsson, L.; Schoneberg, T.; Otto, H.; Hucho, F. Nuclear envelope proteomics: novel integral membrane proteins of the inner nuclear membrane. *Proc. Natl. Acad. Sci. U.S.A.* **2001**, *98* (21), 11943–11948.

(38) Cronshaw, J. M.; Krutchinsky, A. N.; Zhang, W.; Chait, B. T.; Matunis, M. J. Proteomic analysis of the mammalian nuclear pore complex. *J. Cell Biol.* **2002**, *158* (5), 915–927.

(39) Dreger, M. Subcellular proteomics. *Mass Spectrom. Rev.* **2003**, *22* (1), 27–56.

(40) Hansson, O. Biomarkers for neurodegenerative diseases. *Nat. Med.* **2021**, *27* (6), 954–963.

(41) Lleó, A. Biomarkers in neurological disorders: a fast-growing market. *Brain Commun.* **2021**, *3* (2), No. fcab086.

(42) Kawata, K.; Liu, C. Y.; Merkel, S. F.; Ramirez, S. H.; Tierney, R. T.; Langford, D. Blood biomarkers for brain injury: What are we measuring? *Neurosci. Biobehav. Rev.* **2016**, *68*, 460–473.

(43) Alcolea, D.; Beeri, M. S.; Rojas, J. C.; Gardner, R. C.; Lleó, A. Blood Biomarkers in Neurodegenerative Diseases: Implications for the Clinical Neurologist. *Neurology* **2023**, *101* (4), 172–180.